ECORD student research grant findings report: Chemical analyses of IODP 1256D sulphide population by EPMA

Clifford Patten
Department of Geological Sciences.
Stockholm University, Sweden.
clifford.patten@geo.su.se
+46 (0)8 16 4737

Introduction

Hydrothermal fluid circulation in the oceanic crust is an effective mechanism by which energy is released from earth. It is an important geological process that catalyses chemical fluxes between the crust and seawater and can lead to mantle heterogeneities by later subduction (Zindler and Hart, 1986). During fluid circulation the oceanic crust is altered and metals are leached from the deepest rocks which are eventually vented on seafloor as Volcanogenic Massive Sulphide (VMS) deposits enriched in Cu, Zn and Pb (e.g. Pirajno, 2008). Gold, often associated with As, Sb, Se or Te within these deposits (hereafter referred as related elements), can be concentrated enough to form a sub-classification commonly named Au-rich VMS (Mercier-Langevin et al., 2011).

Gold and related elements have been extensively investigated for Mid-Ocean Ridge Basalt (MORB) genesis, oceanic arc formation and mantle processes, and a large database for different tectonic settings exists (Hertogen et al., 1980; Peach et al., 1990; Arevalo and McDonough, 2010; Jenner et al., 2010; Tatsumi et al., 2000; Pitcairn, 2011; Jenner and O'Neill, 2012; Webber et al., 2012). Average MORB content is 0.34ppb Au, 100ppb As, 25ppb Sb, 210ppb Se and 5ppb Te (Webber et al., 2012; Arevalo and McDonough, 2010). Fewer studies have focused on the effect of the hydrothermal alteration on these elements due to the rarity of available samples representative of the whole oceanic crust depth and to the necessity of very low detection limit methods (Keays and Scott, 1976; Nesbitt et al., 1987; Korobeynikov and Pertsev, 1995-1996; Jochum and Verma, 1996). Certainly a gap in knowledge exists in the cycle of these elements in the oceanic crust.

Gold and related elements are chalcophile elements and are preferentially hosted in sulphide minerals in the earth crust (e.g. Barnes and Lightfoot, 2005). In the oceanic crust, Au and related elements are likely to be host in spherical sulphide droplets before the initiation of the hydrothermal alteration (Patten et al.,

2013). Hydrothermal fluid circulation mobilises Au and related elements in the oceanic crust (Patten et al., 2014) which are eventually enriched in VMS on the seafloor (Hannington et al., 1990; Hannington et al., 1999). Consequently the fate of Au and related elements during the hydrothermal alteration of the oceanic crust appears to be closely linked to sulphides and in situ analyses for Au and related elements in sulphide would provide great information.

Integrated Oceanic Drilling Project (IODP) 1256D is an appropriate location to investigate the oceanic crust sulphide population. Situated in the Cocos plate, oceanic crust at IODP 1256D was created from a superfast spreading ridge and gives one of the best insight of the oceanic crust to date with material recovered from the volcanic section to the plutonic complex (Teagle et al., 2006). Moreover the hydrothermal fluid circulation and the alteration fascies resulting are well constrained for a large set of major and trace elements (Wilson et al., 2003; Teagle et al., 2006; Alt et al. 2010; Alt and Shanks, 2011; Violay et al., 2013).

In this study we report a detailed classification of the sulphide population in IODP 1256D. Associated to this classification we also report chemical composition for major elements and few trace elements. Chemical compositions were carried out by Electron Probe Micro-Analyses (EPMA) at Uppsala University. The aim of this study is to determine the major element compositions of the different sulphide phases present in IODP 1256D in order to carry out later in-situ analyses by LA-ICP-MS. Additionally, we also report the distribution of trace elements in the sulphide population of IODP 1256D and the implications on the genesis of these minerals.

Method

Sulphide population classification in IODP 1256D was carried out by reflective microscopy at Stockholm University, Sweden, on 43 thin polished sections. Electron probe micro-analyses have been carried out at Uppsala University, Sweden, with a JXA-8530F JEOL SUPERPROBE. Elements analysed were Fe, S, Cu, Ni, Co, Zn, Pb, As, Se and Mo. An accelerating voltage of 20 kV and a beam current of 20 nA was used for sulphide analyses. Spot analyses were done on different sulphide minerals: pyrite (Py), chalcopyrite (Cpy), pyrrhotite (Po), sphalerite (Sp), pentlandite (Pn), millerite (Mi) and marcasite (Mc). Iron, Se and Mo were calibrated with Astimex standard and S, As, Co, Ni, Pb, Zn and Cu with Cameca standards. Detection limit is set at three sigma and is 105ppm for S, 129ppm for Fe, 228ppm for Cu, 231ppm for Zn, 195ppm for Ni, 174ppm for Co, 231ppm for Se, 438ppm for Pb, 360ppm for As and 243ppm for Mo.

The analyses were done on the 01-08-13, 02-08-13 and 04-03-14 for a cost of 5000sek per day. The total costs are 15000sek or 1654.4eur which are covered by the ECORD student research grant. This grant allowed to make 372 sulphide analyses.

Geological settings

IODP 1256D lithologic units:

Drilling site of IODP 1256D is located in the Cocos Plate (6.736° N, 91.934° W). Basement oceanic crust material was recovered during four expeditions: ODP leg 206, IODP leg 309, 312 and 335. At this location the oceanic crust was created 15Ma ago from a superfast spreading ridge (~200mm/yr; Wilson et al., 2003). It is divided into four main lithological units: the volcanic section, transitional zone, sheeted dyke complex and plutonic complex.

The volcanic section, which extends down to 1004mbsf, is composed of lava ponds and inflated flows on the first 284m of the section. These units were formed during off-axis volcanism events (Teagle et al., 2006). The rest of the section is composed of sheeted flows and massive units. The flows are phyric to aphyric and the massive units are generally aphyric (Teagle et al., 2006). Below the volcanic section the transitional zone extends from 1004 mbsf down to 1061 mbsf and is mainly composed of sheeted flows which are aphyric basalts. The transitional zone is a narrow lithological unit which contains mineralised breccias at 1028 mbsf (Teagle et al., 2006).

The sheeted dyke complex extends from 1061mbsf to 1407mbsf. Massive aphyric basalt is the main lithology (Teagle et al., 2006). Sub-vertical intrusive contacts are common and characterise the dykes. In the lower part, the dykes have granoblastic textures formed by high temperature recrystallization due to the heat released from the underlying gabbros (Teagle et al., 2006). At the bottom of the hole two gabbro bodies penetrated the crust. The upper gabbro is characterised by a complex plagioclase-clinopyroxene-oxides textural relationship interpreted to result from two magmatic episodes (e.g. Teagle et al., 2006). The lower gabbro body consists of medium grained gabbro-gabbronorite characterised by plagioclase, clinopyroxene, orthopyroxene and oxide. The contacts with the dykes are intrusive with dyke fragments in the margin of the body (Alt et al., 2010).

Results

Sulphide population at IODP 1256D:

Based on textural and compositional characteristics observed by optical microscopy a sulphide classification can be made at IODP 1256D. The criteria used are occurrences in lithological units, textures, sizes and mineralogical assemblages. Six main groups can be observed and are shown in Figure 1.

The first group occurs in the volcanic section and is characterized by pyrite-marcasite dominated veins (Fig. 1.1). These veins have been termed "pyrite fronts" and occur on the border of alteration halos (Alt and Shanks, 2011) or oxidation zones (Andrews, 1979). They are believed to form partly from precipitation of remobilized S from oxidized alteration zones. These veins precipitate at low temperature (<150°C) (e.g. Andrews, 1979) and the presence of marcasite indicates acidic solution (<5 pH) and partly oxidized soluble species such as thiosulfate (Murowchick and Barnes, 1986). Such processes are suggested to occur during off-axis fluid circulation.

The second group also occurs in the volcanic section and is characterized by grains of pyrite and chalcopyrite occurring either as disseminated grains in the silicate matrix or in saponite dominated veins. These sulphides are associated to the general low temperature background alteration of the rocks which is related to seawater-derived fluids circulation in the volcanic section (Alt et al., 2010). These sulphides are referred as low temperature sulphides (Fig. 1.2).

The third group occurs in the sheeted dikes and in the transitional zone. The sulphides partly occur in chlorite and quartz dominated veins, as disseminated grains in the rocks or in mineralized breccia (Fig. 1.3). These sulphides precipitated from rising hydrothermal fluids coming from the deep oceanic crust. These fluids have been estimated to have formed at between 320°C and 450°C (Alt et al., 2010) and it is believed that they are responsible for the depletion in Cu and Zn of the lower portion of the core (Alt et al., 2010). Hannington et al., (1990) reported that similar sulphides from mineralised samples of DSDP 504B transitional zone are enriched in Au, As and Sb.

The fourth group is characterized by disseminated sulphides characterized mostly by pyrite and chalcopyrite in the sheeted dyke and the plutonic complex. These sulphides could either be precipitated sulphides from hydrothermal fluids similar to those of group 3 or extensively re-crystallised magmatic sulphides.

The fourth group is characterized by having texture and mineralogical assemblages similar to primary magmatic sulphides and is observed in the volcanic section and the plutonic complex. The criteria for classification as "magmatic" sulphide are a small spherical shape and high temperature phases

characterized by pyrrhotite, chalcopyrite, pentlandite and millerite (Figure 1.4; e.g. Mathez, 1979; Patten et al., 2012). In the plutonic section the magmatic sulphides do not have spherical shapes but still have the same mineral assemblage.

The last group occurs throughout all the lithologic sections and is characterized by some patchy pyrites replacing the silicate matrix and forming spherical shapes and is referred as "patchy" (Fig. 1.5). Their genetic formation is unclear.

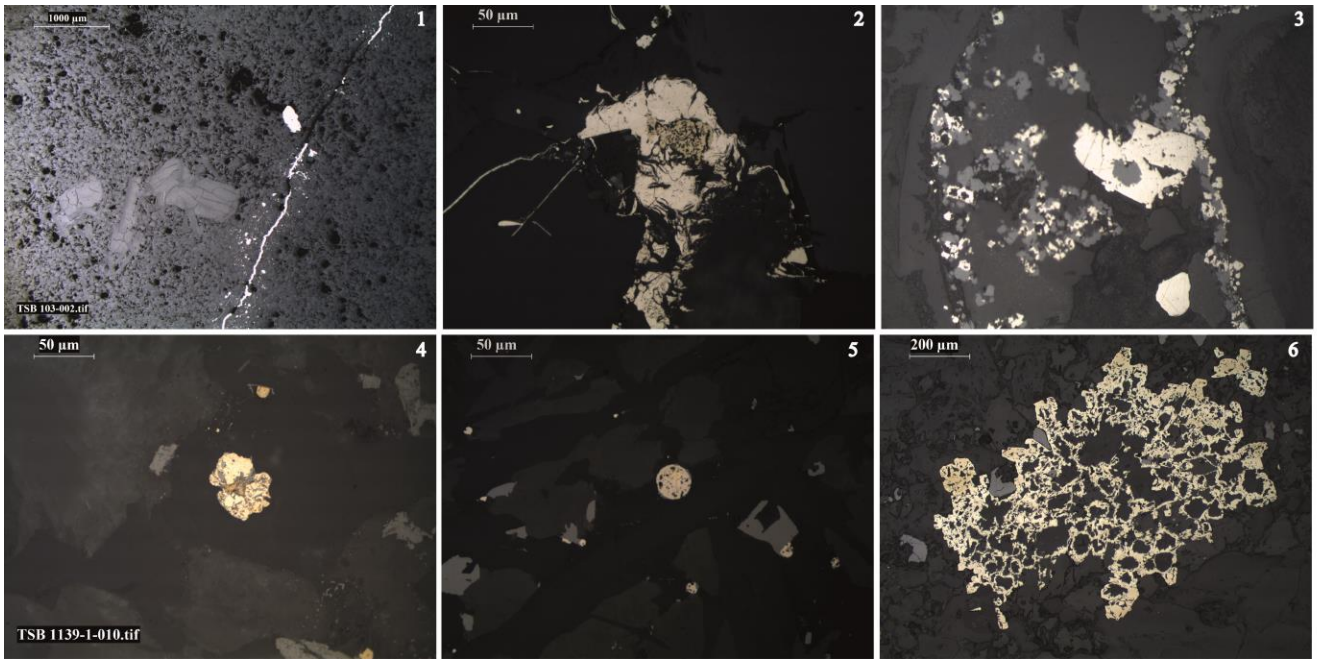

Figure 1. Sulphide population of IODP site 1256D: 1) pyrite front, 2) low temperature sulphides, 3) transitional zone sulphide, 4) high temperature sulphide, 5) primary magmatic sulphide, 6) patchy pyrite.

Chemical composition of the sulphide population in major elements:

Averages of sulphide phases from IODP 1256D are listed in Table 1. Pyrite, chalcopyrite and marcasite have major elements composition in the expected range (Table 1). Pyrrhotite has a low Fe content (58.2±1.33% instead of 62.3%) and a high S content (39.4±0.5% instead of 37.9%); it also contains up to 0.97±0.8%Ni. Sphalerite has a high content in Fe (8.53±1.33% instead of 2.88%) and a low Zn content (55.2±0.03% instead of 64.06%). Pentlandite and millerite have low Ni content (21.5±4.01% and 51.3±12.25%, respectively instead of 34.21% and 64.67%, respectively) and high Co content (16.49±3.93% and 5.61±7.42%, respectively).

		As	Se	S	Co	Ni	Pb	Mo	Zn	Fe	Cu	Total
Pyrite	n=176	0.006	0.013	53.2	0.18	0.19	0.38	0.59	0.01	46.22	0.07	100.9
	σ		0.00	0.8	0.68	0.43	0.03	0.03	0.04	1.01	0.68	1.10
Chalcopyrite	n=70	0.006	0.014	35.2	0.04	0.16	0.30	0.43	0.06	31.00	32.38	99.6
	σ		0.020	1.7	0.14	0.39	0.04	0.03	0.19	1.73	3.10	1.05
Pyrrhotite	n=27	0.006	0.014	39.4	0.11	0.97	0.32	0.46	0.01	58.21	0.05	99.6
	σ		0.019	0.5	0.21	0.80	0.03	0.02	0.03	1.33	0.19	1.54
Sphalerite	n=18	0.006	0.014	33.7	0.01	0.00	0.30	0.43	55.23	8.53	1.28	99.5
	σ		0.019	0.5	0.21	0.80	0.03	0.02	0.03	1.33	0.19	1.54
Pentlandite	n=5	0.006	0.028	42.0	16.49	21.49	0.03	0.49	0.00	19.85	0.00	100.3
	σ		0.023	0.4	3.93	4.01	0.05	0.01	0.00	6.36	0.00	0.68
Millerite	n=7	0.006	0.074	38.2	5.61	51.26	0.00	0.44	0.01	4.01	0.37	101.0
	σ		0.034	3.5	7.42	12.25	0.00	0.03	0.01	1.88	1.04	0.89
Marcasite	n=7	0.006	0.007	53.2	0.00	0.03	0.41	0.59	0.01	46.77	0.01	100.0
	σ		0.01	0.3	0.00	0.01	0.03	0.03	0.02	0.16	0.00	0.25

Table 1: Average composition of sulphides in IODP 1256D. Values are in weight percent. σ= standard deviation.

Trace elements in the sulphide population:

Trace elements average concentrations in the sulphide population of IODP 1256D are showed in Figure 2:

- Selenium: Pentlandite and millerite have the highest content in Se (280±231.4ppm and 741±341ppm, respectively). Chalcopyrite, pyrrhotite and sphalerite have Se content slightly above detection limit whereas pyrite and marcasite are at or below detection limit.
- Cobalt: Cobalt is a major element in pentlandite and millerite; it is also present as trace in the pyrite, chalcopyrite and pyrrhotite whereas it is below detection limit for sphalerite and marcasite.
- Nickel: Nickel is also a major element in pentlandite and millerite; it is also present as trace element in pyrite, chalcopyrite and mostly in pentlandite. It is close to detection limit in sphalerite and marcasite.
- Zinc: Zinc is a major element in sphalerite. It is also present as traces in chalcopyrite. Zinc content in other minerals is at or below detection limit.
- Copper: Copper is a major element in chalcopyrite. Sphalerite has 1.2±0.%1 Cu which can be attributed to contamination from chalcopyrite by secondary X-ray diffraction in sphalerite grains having a chalcopyrite disease texture. Sphalerites without chalcopyrite disease texture have 0.2±0.2%Cu. Trace Cu is also present in millerite pyrite and pyrrhotite. Copper content in pentlandite and marcasite is below detection limit.
- Led: Led is present as trace element in pyrite, chalcopyrite, pyrrhotite, sphalerite and marcasite. It is below detection limit in pentlandite and millerite. Marcasite and pyrite have the highest Pb content with 0.41±0.03% and 0.37±0.03%, respectively.
- Arsenic: Arsenic content in all minerals is below detection limit.
- Molybdenum: Molybdenum concentration in constant in the different sulphide minerals and ranges between 0.43% and 0.59%.

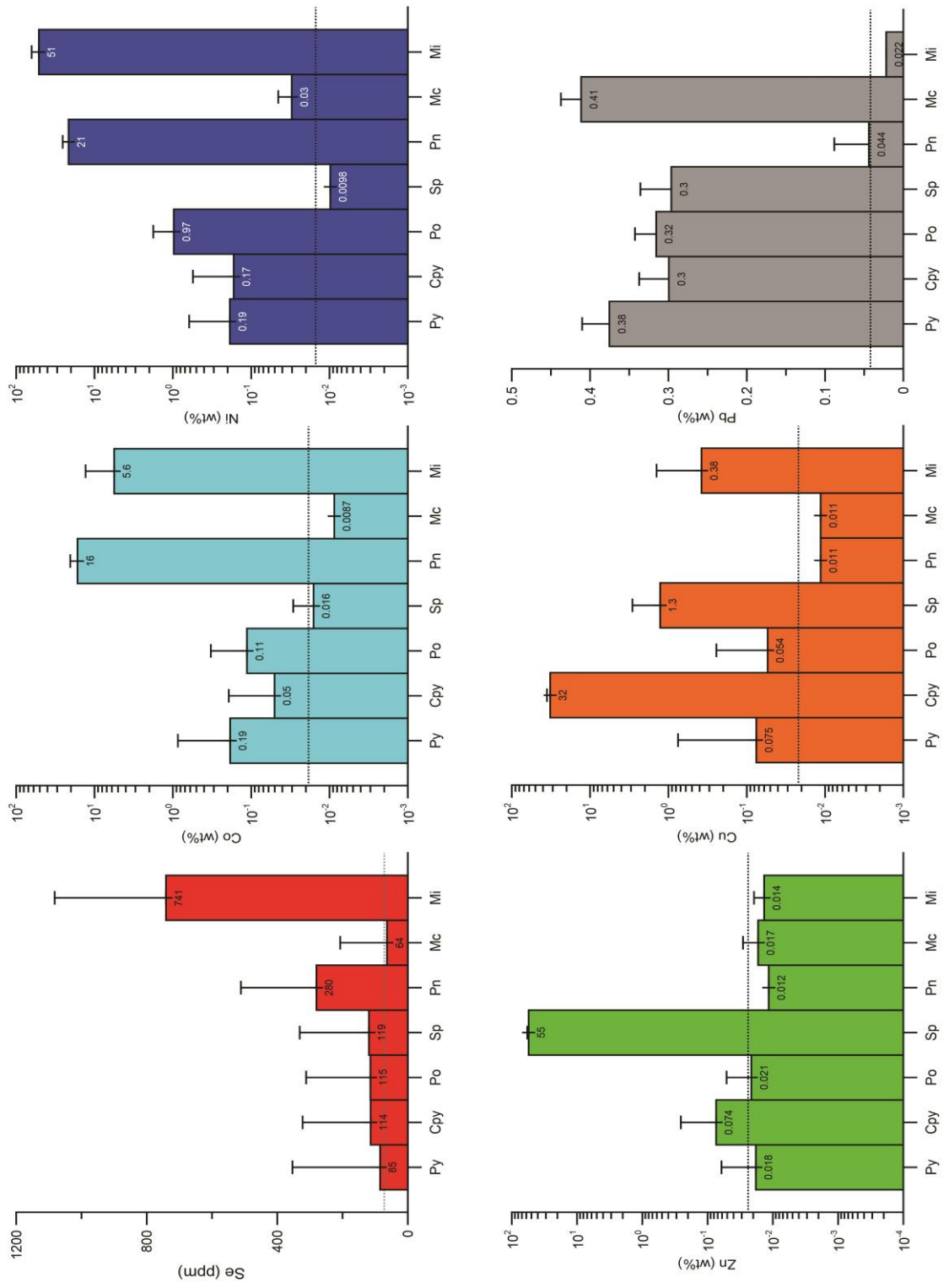

Figure 2. Trace elements in IODP 1256D sulphide population. Dashed lines are detection limits.

Trace elements in Pyrite

Pyrite is the only sulphide minerals present in all the different group of sulphides. Trace element concentrations in pyrite are shown in Figure 3. Selenium is generally below detection limit in pyrite except for few grains in the transitional zone and in the remobilised pyrite group. Cobalt and nickel have a similar behaviour in pyrite: they are more concentrated in magmatic related, high temperature and patchy pyrites than in the other groups. Zinc concentration in pyrites is mostly below detection limit except for few grains from the high temperature and transitional zone group. Only magmatic related pyrites have Cu content above detection limit. Led is homogeneously distributed in all the different type of pyrites.

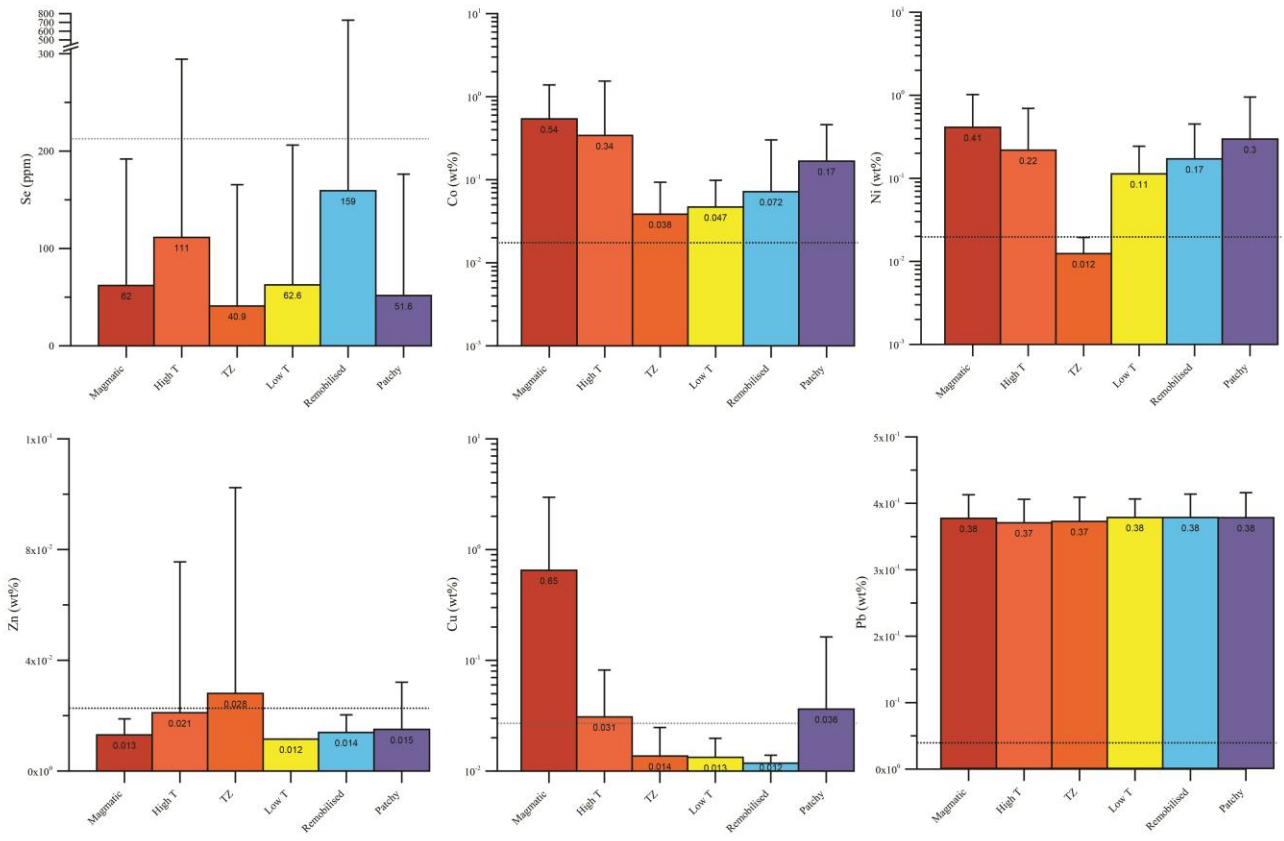

Figure 3. Trace elements in pyrites. Dashed lines are detection limits.

Discussion

Major elements:

Analyses by EPMA of the sulphide population of IODP 1256D enabled to accurately determine the concentration of major elements. Most of the sulphide minerals have major elements composition in the range. Sphalerite has high Fe content (up to 12.3%) which is not surprising as its concentration is highly

variable (6-25%) in hydrothermal vent sphalerites (Scott, 1983 and reference in there). At high pressure, Fe content in sphalerite can be used as a geobarometer but is affected by metamorphism. Copper disease in sphalerite is one effect of the metamorphism (Scott, 1983; Lepetit et al., 03) and is common in sphalerite from IODP 1256. Thus, the use of Fe content in sphalerite in IODP 1256D for geobarometry is not recommended.

Pentlandite and millerite can have high concentrations of Co (up to 20.9% and 14.8%, respectively). Kaneda et al. (1986) determined stability fields of pentlandite in the Fe-Ni-Co-S system at different temperatures. The pentlandite compositions of IODP 1256D are in the stability field of pentlandite at 300ºC or higher. This order of magnitude is similar to that determined by Alt et al. (2010) in IODP 1256D for the plutonic section where pentlandite is present.

Trace elements:

Cobalt and Ni are also present as trace elements in pyrrhotite and pyrite and in pentlandite and millerite for Co. Cobalt to Ni ratios in pyrrhotite, pentlandite and millerite are shown in Figure 4. During fractional crystallisation in ultramafic and mafic rocks, Ni is preferentially taken by olivine than Co resulting in an increasing Co/Ni differentiation trend in the sulphides which form from the melt (Merkle and Von Gruenewaldt, 1986). Such phenomenon is observed in fresh MORB sulphide droplets (Figure 4; Patten et al., 2013). In fresh MORB sulphide droplets, the Co/Ni is similar in the pyrrhotite and pentlandite phases from the same sulphide droplets (Figure 4). Cobalt to Ni ratio in IODP 1256D pyrrhotites plots on the fresh MORB sulphide droplets differentiation trend confirming their magmatic origin (Figure 4). Although pyrrhotites have magmatic origins they might have been re-crystallised due to hydrothermal fluid circulation. Indeed, numerous pyrrhotite grains have slightly low Co concentration and are associated with pentlandite grains which have extremely high Co concentrations relatively to fresh MORB pentlandite (Figure 4). These are Co-rich pentlandite. Merkle and Von Gruenewaldt (1986) reported those magmatic Co-rich pentlandites can exsolve from sulphides which in turn exsolved from Ni-depleted silicate melt; however, they also highlighted correlations between Co/Ni in pyrrhotite and pentlandite. We suggest that Cobalt-rich pentlandite from IODP 1256D are not primary magmatic sulphides as they do not have similar Co/Ni ratio to that of their corresponding pyrrhotite (Figure 4) and that the silicate melt from which sulphides exsolved is not expected to be Ni-poor. We speculate, however, that primary pyrrhotite and pentlandite from IODP 1256D had Co to Ni ratio similar to fresh MORB sulphides but that they sustained re-crystallisation during which Co diffused from the pyrrhotite into pentlandite to form Co-rich pentlandite. Because pyrrhotite and pentlandite in IODP 1256D still have magmatic textures we expect that the amount of re-crystallisation is minor.

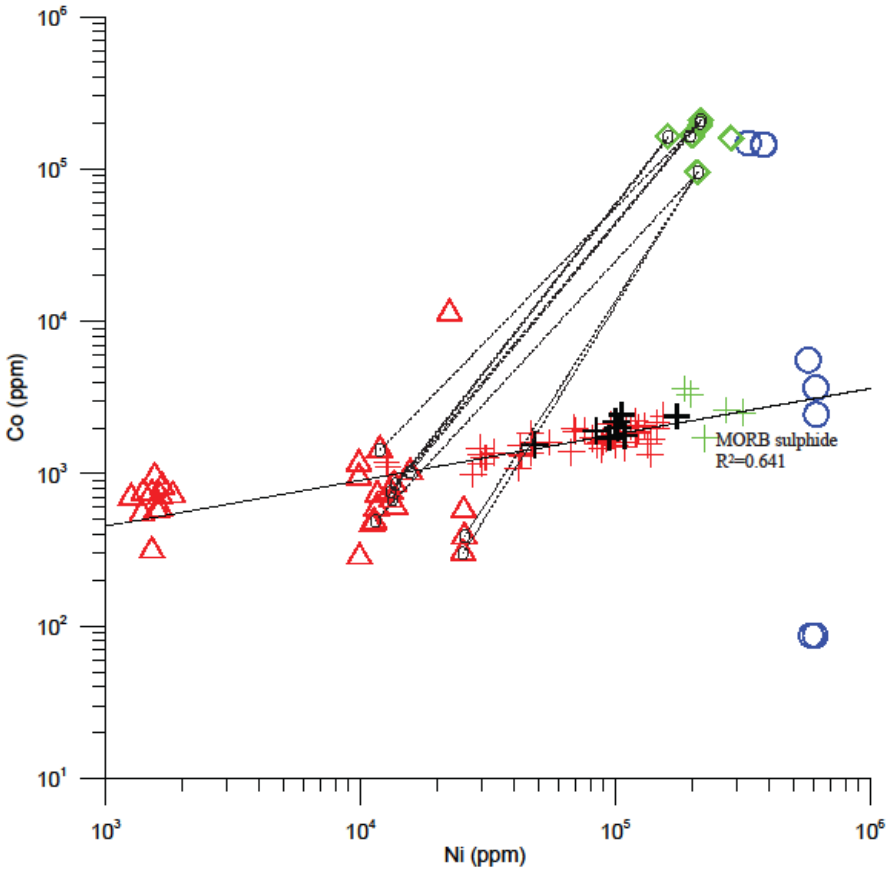

Figure 4. Cobalt and Ni concentrations in pyrrhotite, pentlandite and millerite. Red triangles are pyrrhotites, green squares are pentlandites and blue circles are millerites. Fresh MORB sulphide droplets Co and Ni concentrations are also plotted (Patten et al., 2013): black crosses are bulk sulphide droplets values, red crosses are pyrrhotite sulphide droplets values and green crosses are pentlandite sulphide droplets values. Differentiation curves is calculated from the fresh sulphide droplets values. Dashed lines represent related pyrrhotite and pentlandite from IODP 1256D.

Cobalt to Ni ratio has been also used in pyrite as a geochemical tool for ore deposits discrimination (Bralia et al., 1979; Bajwah et al., 1987). Cobalt to Ni ratio in pyrites is shown in Figure 5. Distinctive area for pyrites from different sulphide groups can be observed relative to their Co/Ni: pyrites from the transitional zone sulphide group have the highest Co/Ni, this range is similar to those of exhalative submarine deposits (Bajwah et al., 1987); pyrites from low temperature and patchy sulphide group have similar Co/Ni ratio; finally, pyrite from pyrite front group have the lowest Co/Ni ratio. Pyrites from the high temperature sulphide group do not have a specific distribution. High temperature sulphides are present in the sheeted dykes and in the plutonic section and they can either be precipitates from hydrothermal fluids or re-crystallised primary sulphide. Those which are present in veins, however, have surely precipitated from

fluids have similar Co/Ni that sulphides from the transitional zone (Figure 4). Two possible parameters have a control the Co/Ni in precipitated pyrites: the temperature and the oxygen fugacity.

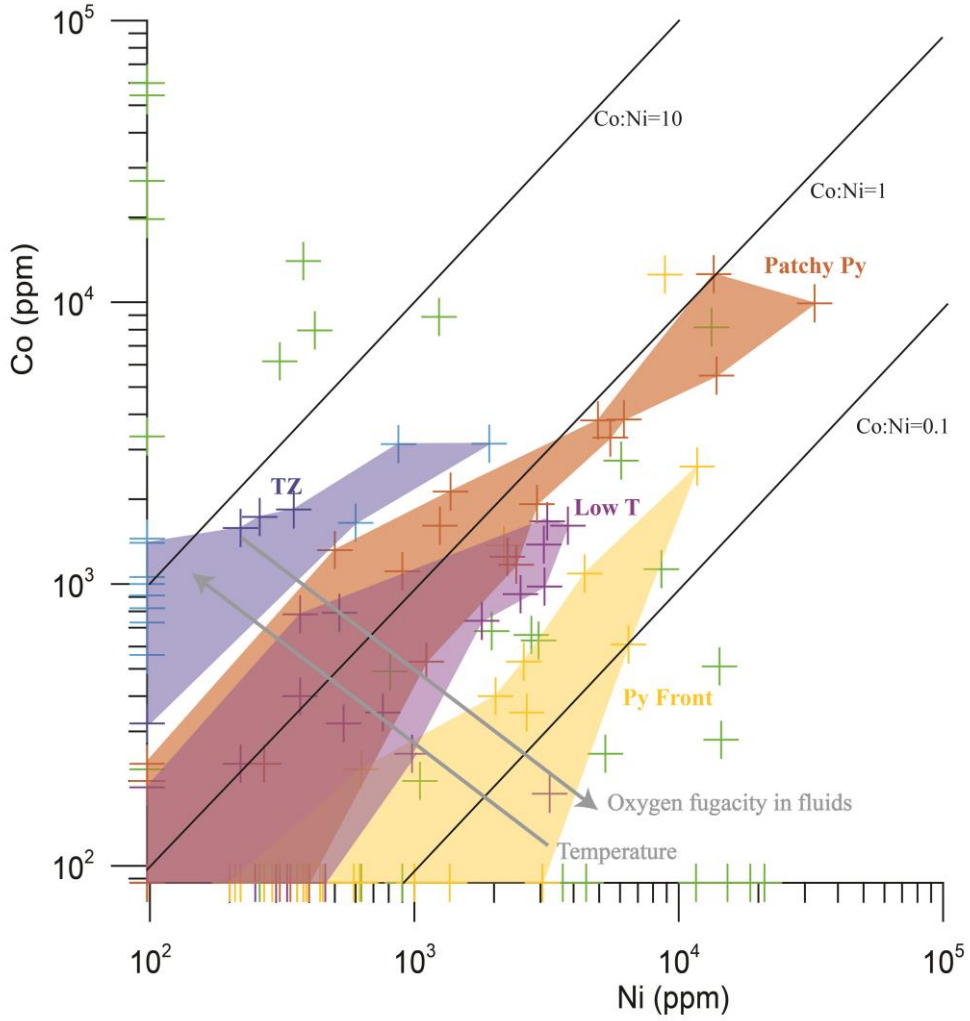

Figure 5. Cobal and Ni concentrations from pyrites. Yellow crosses represent patchy pyrite, purple ones represent low temperature pyrite, blue one represent transitional zone pyrite, green ones represent high temperature ones and brown ones represent patchy pyrite.

In chalcopyrite, Co and Ni are also present as trace elements up to 1.08% and 1.61%, respectively. Figure 5 shows Co+Ni concentration in chalcopyrite relative to the Cu concentration. It appears that there is a negative correlation between Co+Ni and Cu suggesting that Co and Ni can substitute for Cu in the chalcopyrite lattice. This substitution is independent of the type of sulphide group.

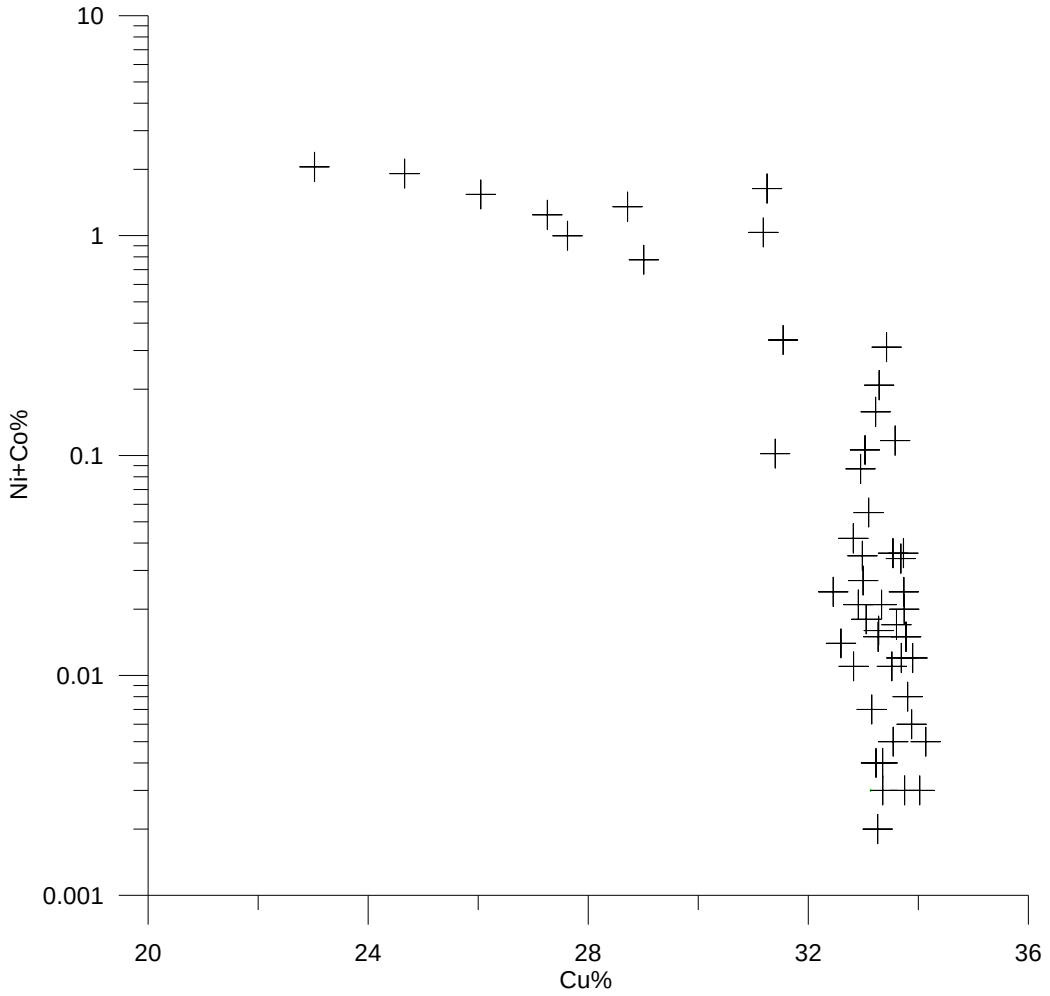

Figure 6. Nickel and Co concentration in chalcopyrite.

Conclusion

Analyses by EPMA of IODP 1256D sulphide population enable to determine the major element compositions of the different sulphide phases. Major elements composition is needed for later in-situ analyses by LA-ICP-MS in order to do proper calibration. Moreover, EPMA analyses also enable to determine trace element compositions of the different sulphide phases and to highlight their specific distribution:

1. Pyrite, chalcopyrite, pyrrhotite and marcasite have an expected major element compositions. Sphalerite has high Fe content and pentlandite and millerite have high Co content.
2. Selenium is enriched in millerite and pentlandite relative to the other sulphide phases.
3. Arsenic is below detection limit for all the sulphide phases.
4. Led is enriched in marcasite and pyrite relative to the other sulphide phases.

5. Cobalt to Ni ratio in pyrrhotite and pentlandite highlight their magmatic origin. It also suggests that they have been partially re-crystallised and that Co migrated from the pyrrhotite to the pentlandite.
6. Precipitated pyrites from fluids have distinctive Co/Ni depending on their sulphide groups. The ratio is likely to be controlled by temperature or oxygen fugacity.

References

Alt, J.C., Laverne, C., Coggon, R.M., Teagle, D.A.H., Banerjee, N.R., Morgan, S., Smith-Duque, C.E., Harris, M., Galli, L., 2010. Subsurface structure of a submarine hydrothermal system in ocean crust formed at the East Pacific Rise, ODP/IODP Site 1256. Geochemistry, Geophysics and Geosystems, 11(10).

Alt, J.C., Shanks, W.C., 2011. Microbial sulfate reduction and the sulfur budget for a complete section of altered oceanic basalts, IODP Hole 1256D (eastern Pacific). Earth and Planetary Science Letters 310, 73-83.

Andrews, A.J., 1979. On the effect of low-temperature seawater-basalt interaction on the distribution of sulfur in oceanic crust, layer 2. Earth and Planetary Science Letters 46, 68-80.

Arevalo, R., McDonough, W.F., 2010. Chemical variations and regional diversity observed in MORB. Chemical Geology 271, 70-85.

Bajwah, Z., Seccombe, P., Offler, R., 1987. Trace element distribution, Co: Ni ratios and genesis of the Big Cadia iron-copper deposit, New South Wales, Australia. Mineralium Deposita 22, 292-300.

Barnes, S.J., Lightfoot, P.C., 2005. Formation of magmatic nickel-sulfide ore deposits and processses affecting their copper and platinum-group element contents. Economic Geology 100th Anniversary Volume, 179-213.

Bralia, A., Sabatini, G., Troja, F., 1979. A revaluation of the Co/Ni ratio in pyrite as geochemical tool in ore genesis problems. Mineralium Deposita 14, 353-374.

Jenner, F.E., O'Neill, H.S.C., Arculus, R.J., Mavrogenes, J.A., 2010. The magnetite crisis in the evolution of arc-related magmas and the initial concentration of Au, Ag and Cu. Journal of Petrology 51, 2445-2464.

Jochum, K., Verma, S., 1996. Extreme enrichment of Sb, Tl and other trace elements in altered MORB. Chemical Geology 130, 289-299.

Hannington, M.D., Herzig, P.M., Alt, J.C., 1990. The distribution of gold in sub-seafloor stockwork mineralization from DSDP hole 504B and the Agrokipia B deposit, Cyprus. Canadian Journal of Earth Sciences 27, 1409-1417.

Hannington, M.D., 1999. Volcanogenic gold in the massive sulfide environment volcanic-associated massive sulfide deposits: Processes and examples in modern and ancient settings. Reviews in Economic Geology 8, 325-356.

Hertogen, J., Janssens, M.J., Palme, H., 1980. Trace elements in ocean ridge basalt glasses: implications for fractionations during mantle evolution and petrogenesis. Geochimica et Cosmochimica Acta 44, 2125-2143.

Jenner, F.E., O'Neill, H.S., 2012. Analysis of 60 elements in 616 ocean floor basaltic glasses. Geochemistry, Geophysics and Geosystems, 13.

Kaneda, H., Takenouchi, S., Shoji, T., 1986. Stability of pentlandite in the Fe-Ni-Co-S system. Mineralium Deposita 21, 169-180.

Keays, R.R., Scott, R.B., 1976. Precious metals in ocean-ridge basalts; implications for basalts as source rocks for gold mineralization. Economic Geology 71, 705-720.

Korobeynikov, A.F., and Pertsev, N.N., 1995. Distribution of Au and Pd in basalts and diabases in Hole 504B, Leg 69 and Leg 140. *In* Erzinger, J., Becker, K., Dick, H.J.B., and Stokking, L.B. (Eds.), *Proc. ODP, Sci. Results*, 137/140, 117-120.

Korobeynikov, A.F., Pertsev, N.N., 1996. Data report: gold content in upper crustal rocks from hole 504B1.

Lepetit, P., Bente, K., Doering, T., Luckhaus, S., 2003. Crystal chemistry of Fe-containing sphalerites. Physics and chemistry of minerals 30, 185-191.

Merkle, R.K., von Gruenewaldt, G., 1986. Compositional variation of Co-rich pentlandite; relation to the evolution of the upper zone of the western Bushveld Complex, South Africa. The Canadian Mineralogist 24, 529-546.

Mathez, E.A., 1979. Sulfide relations in hole 418a flows and sulfur contents of glasses. Initial reports of the Deep Sea Drilling Project 51, 1069-1085.

Mercier-Langevin, P., Hannington, M.D., Dube, B., Becu, V., 2011. The gold content of volcanogenic massive sulfide deposits. Mineralium Deposita 46, 509-539.

Nesbitt, B.E., St. Louis, R.M., Muehlenbachs, K., 1987. Distribution of gold in altered basalts of DSDP hole 504B. canadian journal of earth sciences 24, 201-209.

Patten, C., Barnes, S.-J., Mathez, E.A., 2012. Textural variations in MORB sulfide droplets due to differences in crystallization history. Canadian Mineralogist 50, 675-692.

Patten, C., Barnes, S.-J., Mathez, E.A., Jenner, F.E., 2013. Partition coefficients of chalcophile elements between sulfide and silicate melts and the early crystallization history of sulfide liquid: LA-ICP-MS analysis of MORB sulfide droplets. Chemical Geology 358, 170-188.

Patten, C., Pitcairn, I.K., 2014. Behaviour of Au, As, Sb, Se and Te during the hydrothermal alteration of the oceanic crust: a study case from IODP site 1256D. Nordic Geological Winter Meeting 2014.

Peach, C.L., Mathez, E.A., Keays, R.R., 1990. Sulfide Melt Silicate Melt Distribution Coefficients for Noble-Metals and Other Chalcophile Elements as Deduced from MORB - Implications for Partial Melting. Geochimica et Cosmochimica Acta 54, 3379-3389.

Pitcairn, I.K., 2011. Background concentrations of gold in different rock types. Applied Earth Science 120, 31-38.

Pirajno, F., 2008. Hydrothermal Processes and Mineral Systems. Springer.

Scott, S., 1983. Chemical behaviour of sphalerite and arsenopyrite in hydrothermal and metamorphic environments. Mineralogical Magazine 47, 427-435.

Tatsumi, Y., Oguri, K., Shimoda, G., Kogiso, T., Barsczus, H.G., 2000. Contrasting behavior of noble-metal elements during magmatic differentiation in basalts from the Cook Islands, Polynesia. Geology 28, 131-134.

Teagle, D.A.H., Alt, J.C., Umino, S., Miyashita, S., Banerjee, N.R., Wilson, D.S., 2006. Expedition 309/312 Scientists. Superfast Spreading Rate Crust 2 and 3. Proc. IODP, 309/ 312.

Violay, M., Pezard, P.A., Ildefonse, B., Célérier, B., Deleau, A., 2012. Structure of the hydrothermal root zone of the sheeted dikes in fast-spread oceanic crust: a core-log integration study of ODP hole 1256D, Eastern Equatorial Pacific. Ofioliti 37, 1-11.

Webber, A.P., Roberts, S., Taylor, R.N., Pitcairn, I.K., 2013. Golden plumes: Substantial gold enrichment of oceanic crust during ridge-plume interaction. Geology 41, 87-90.

Wilson, D.S., et al., 2003. Proceedings of the Ocean Drilling Program, Initial Reports, vol. 206. Ocean Drill. Program, College Station, Tex.

Zindler, A., and S. R. Hart, 1986. Chemical geodynamics. Annual Review of Earth and Planetary Sciences 14, 115-118.